Siew Yee Lim, Cheryl Suwen Law, Abel Santos

Surface modification of nanoporous anodic alumina photonic crystals for photocatalytic applications

Proceedings of SPIE Nanophotonics Austalasia, 2018 / vol.10456, pp.1045658-1-1045658-9

Originally published at: http://dx.doi.org/10.1117/12.2282248

Surface modification of nanoporous anodic alumina photonic crystals for photocatalytic applications

Lim, Siew Yee, Law, Cheryl Suwen, Santos, Abel

Siew Yee Lim, Cheryl Suwen Law, Abel Santos, "Surface modification of nanoporous anodic alumina photonic crystals for photocatalytic applications," Proc. SPIE 10456, Nanophotonics Australasia 2017, 1045658 (2 January 2018); doi: 10.1117/12.2282248

SPIE.

Event: SPIE Nanophotonics Australasia, 2017, Melbourne, Australia

Surface Modification of Nanoporous Anodic Alumina Photonic Crystals for Photocatalytic Applications

Siew Yee Lim[a,b,c], Cheryl Suwen Law[a,b,c], Abel Santos[a,b,c*]

[a] School of Chemical Engineering, The University of Adelaide, Australia; [b] Institute for Photonics and Advanced Sensing (IPAS), The University of Adelaide, Australia; [c] ARC Centre of Excellence for Nanoscale Biophotonics (CNBP), The University of Adelaide, Australia
*abel.santos@adelaide.edu.au

ABSTRACT

Herein, we report on the development of a rationally designed composite photocatalyst material by combining nanoporous anodic alumina-rugate filters (NAA-RFs) with photo-active layers of titanium dioxide (TiO_2). NAA-RFs are synthesised by sinusoidal pulse anodisation and subsequently functionalised with TiO_2 by sol-gel method to provide the photonic structures with photocatalytic properties. We demonstrate that the characteristic photonic stopband (PSB) of the surface-modified NAA-RFs can be precisely tuned across the UV-visible-NIR spectrum to enhance the photon-to-electron conversion of TiO_2 by 'slow photon effect'. We systematically investigate the effect of the anodisation parameters (i.e. anodisation period and pore widening time) on the position of the PSB of NAA-RFs as well as the photocatalytic performances displayed by these photonic crystal structures. When the edges of the PSB of surface-modified NAA-RFs are positioned closely to the absorption peak of the model organic dye (i.e. methyl orange – MO), the photocatalytic performance of the system to degrade these molecules is enhanced under simulated solar light irradiation due to slow photon effect. Our investigation also reveals that the photocatalytic activity of surface-modified NAA-RFs is independent of slow photon effect and enhances with increasing period length (i.e. increasing anodisation period) of the photonic structures when there is no overlap between the PSB and the absorption peak of MO. This study therefore provides a rationale towards the photocatalytic enhancement of photonic crystals by a rational design of the PSB, creating new opportunities for the future development of high-performance photocatalysts.

Keywords: Photocatalysis, nanoporous anodic alumina, photonic stopband, photonic crystal, anodisation, solar light, photolysis

1. INTRODUCTION

Organic dyes are commonly discharged to water sources or ecosystems from various industries, including textile, cosmetic, pharmaceutical, food, paper, plastic and printing[1-2]. These untreated dyes may be highly reactive and persistent when released to the environment, preventing the absorption of solar light required by the aquatic plants for photosynthesis, deteriorating the aquatic ecosystems and the quality of water sources[3-6]. Conventional chemical and biological water treatment processes (coagulation, flocculation, clarification, filtration, and disinfection) cannot effectively remove these emerging pollutants to meet the stringent water quality standards. Therefore, cost-competitive, eco-friendly wastewater treatments are urgently needed. Among the different alternatives, heterogeneous photocatalysis (henceforth "photocatalysis") is a light-driven process that harnesses solar energy to generate strong, oxidising and non-selective radicals (i.e. ·OH radicals) on the surface of semiconductor materials to mineralise organic pollutants to harmless compounds for the environment and humans[7].

An example of a key photo-active material for photocatalysis is titanium dioxide (TiO_2). This semiconductor has excellent photochemical stability and well-balanced electrochemical properties for good photocatalytic activities[7-8]. However, its intrinsic limitations in light absorption (i.e. constrained to UV light, which is only ~5% of the solar

Nanophotonics Australasia 2017, edited by James W. M. Chon, Baohua Jia, Proc. of SPIE
Vol. 10456, 1045658 · © 2018 SPIE · CCC code: 0277-786X/18/$18 · doi: 10.1117/12.2282248

spectrum) and high recombination rate of photogenerated charge carriers constrain the efficient solar-to-energy conversion in TiO_2-based photocatalysts[9-11]. In addition, the practical use of TiO_2 as nanoparticles presents difficulties in the recovery of the nanoparticles[12-14], including low adsorption capacity[13-15], high aggregation tendency[16] and potential toxicity when released to the environment[17]. Therefore, enhancement of solar-to-energy conversion and immobilisation of TiO_2 are required to address these problems.

The macroscopic optoelectronic properties of semiconductors are strongly dependent on the interaction between photons (light) and atoms (matter) at the nanoscale. In light-driven processes, every photon is precious and, as such, a rational management of photons can lead to efficient photon-to-electron conversions for enhanced optoelectronic applications. Smart designs of materials at the nanoscale can lead to high-performance photocatalyst materials by efficient solar-to-energy (photon-to-electron) conversions. Photonic crystal (PC) structures are periodic optical nanostructures that can control the propagation of light when incoming photons travel across the PCs' structures[18-22]. In particular, nanoporous PC structures possess unique structural and optical properties to facilitate mass transfer and light utilisation[23-24] through their large surface area to volume ratio and slow photon (SP) effects[25]. The rational utilisation of SP effects can improve the photocatalytic activities of photocatalyst materials by tuning the PC's photonic stopband (PSB) and overlap it with the absorption of organic dyes[25-26]. The structural engineering of the PSB of nanoporous PCs [27] can slow down incoming photons at its edges and localise them in the photo-active material to increase the photogeneration of charge carriers[26].

Nanoporous anodic alumina (NAA) produced by anodisation of aluminium is envisaged as a platform to develop PC structures due to its highly controllable and flexible nanopore geometry, chemical resistance, thermal stability, mechanical robustness and optoelectronic properties[28-29]. Some examples of PC structures of NAA include optical microcavities, Fabry-Perot interferometers, bandpass filters, distributed Bragg reflectors, gradient-index filters[27] and rugate filters (RFs)[30]. Among these, NAA-RFs feature a well-resolved intense characteristic PSB, which can be readily tuned across the spectral regions to match the absorption bands of environmental pollutants. Another advantage of NAA-RFs is that the inner surface of these PCs can be modified with layers of photo-active materials to endow NAA-RFs with photocatalyst properties[31].

In this context, this study aims to use NAA-RFs as a platform material to enhance the photocatalytic performances of TiO_2. NAA-RFs are produced by galvanostatic sinusoidal pulse anodisation and subsequently functionalised with photo-active layers of TiO_2 through sol-gel method (Fig. 1). We demonstrate that the position of the characteristic PSB of the NAA-RFs can be precisely engineered by systematically modifying the anodisation period and pore widening time. The effect of these anodisation parameters on the PSB of the photonic structures as well as the photocatalytic degradation of a model dye (i.e. methyl orange – MO) are systematically evaluated.

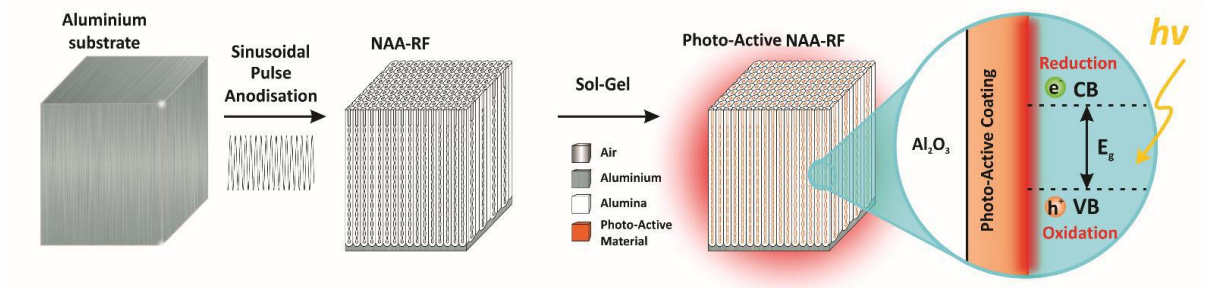

Figure 1. Scheme describing the fabrication of photo-active NAA-RF from its precursor (aluminium substrate) by sinusoidal pulse anodisation (left) and sol-gel method (right).

2. EXPERIMENTAL

2.1 Fabrication of NAA-RFs by sinusoidal pulse anodisation

NAA-RFs were synthesised by galvanostatic sinusoidal pulse anodisation (SPA) approach using and aqueous sulphuric acid (H_2SO_4) electrolyte (Fig. 2) as described by Santos et al.[30]. Briefly, 1.5 x 1.5 cm^2 aluminium (Al) substrates were

sonicated in ethanol (EtOH) and water each for 15 min to remove organic residues. These Al substrates were electropolished in a mixture of EtOH and perchloric acid ($HClO_4$) 4:1 (v:v) at 20 V and 5 °C for 3 min. The electropolished Al substrates were anodised using a 1.1 M aqueous H_2SO_4 solution, in which 25 v% EtOH was added to prevent it from freezing at temperatures below 0 °C[32-33]. The anodisation process was started for 1 h at -1 °C with a constant current density of 1.12 mA cm^{-2} to produce a thin layer of nanoporous oxide that acts as a shuttle to achieve homogeneous pore growth before SPA. The anodisation profile was subsequently set to sinusoidal pulse mode, where the current density was sinusoidally pulsed between high (J_{Max} = 1.12 mA cm^{-2}) and low (J_{Min} = 0.28 mA cm^{-2}) current density values, according to equation (1):

$$J(t) = A_J\left[\sin\left(\frac{2\Pi}{T_P}t\right)+1\right] + J_{Offset} \quad (1)$$

For this equation, $J(t)$ is the current density at a given time t, A_J is the current density amplitude, T_P is the anodisation period and J_{Offset} is the current density offset (Fig. 2).

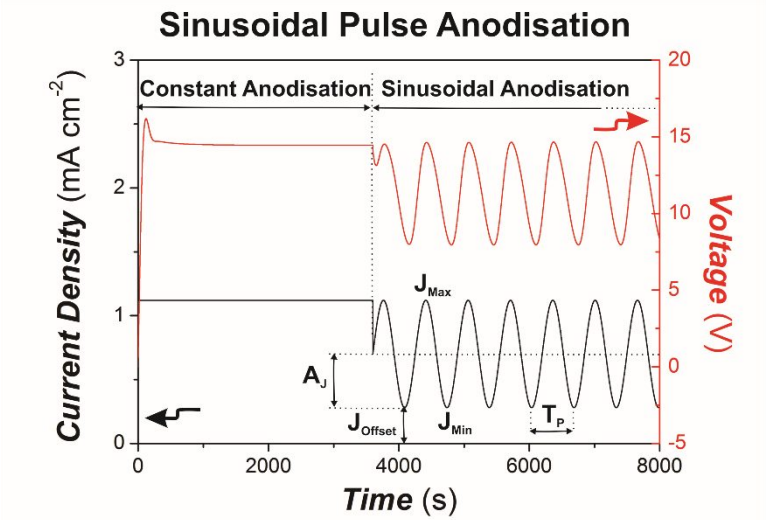

Figure 2. Representative anodisation profile used to produce NAA-RFs including a graphical description of the main anodisation parameters (i.e. T_P, J_{Min}, J_{Max}, J_{Offset} and A_J).

Certain anodisation parameters were fixed for SPA as follows: the current density amplitude (A_J = 0.420 mA cm^{-2}), current density offset (J_{Offset} = 0.28 mA cm^{-2}) and total anodisation time (t_{An} = 20 h). To engineer the photonic features of NAA-RFs (i.e. characteristic transmission peaks or PSB), the anodisation period (T_P) and pore widening time (t_{pw}) were systematically modified from 650 to 850s (ΔT_P = 100 s) and from 0 to 6 min (Δt_{pw} = 2 min), respectively.

Before pore widening was carried out, the remaining aluminium substrate from the backside of NAA-RFs was removed by wet chemical etching in a saturated solution of hydrochloric acid-copper (II) chloride ($HCl–CuCl_2$), using a 5 mm diameter circular window etching mask. Subsequently, the nanopores of NAA-RFs were widened in an aqueous phosphoric acid (H_3PO_4 5 wt %) solution by wet chemical etching at 35 °C for the pore widening time specified (from 0 to 6 min with Δt_{pw} = 2 min).

2.2 Surface modification of NAA-RFs with TiO_2

The inner surface of NAA-RFs produced with different T_p (650, 750 and 850 s) at fixed t_{pw} (6 min) was modified with photo-active layers of TiO_2 through sol-gel method[34]. TiO_2 sol was prepared by magnetically stirring a mixture of titanium (IV) butoxide (3 mol %) and EtOH (97 mol %) in a beaker for 10 min. NAA-RFs were subsequently dip coated by immersing them into TiO_2 sol for 24 h. The surface-modified NAA-RFs were washed with EtOH to remove any excess sol and titanium (IV) butoxide on the surface. These samples were dried in an oven at 50 °C for 10 min to evaporate any residual EtOH.

2.3 Optical characterisation

The transmission spectra of NAA-RFs in air were obtained across the UV-visible spectrum (i.e. from 200 to 800 nm) at normal incidence (i.e. $\theta = 0^o$) using a UV-visible spectrophotometer (Cary 300, Agilent, USA). The transmission spectra of the surface-modified NAA-RFs in air and 5 mg L^{-1} of MO were also collected under the same conditions. Digital images of NAA-RFs displaying interferometric colours were acquired by using a Canon EOS 700D digital camera equipped with a Tamron 90 mm F2.8 VC USD macro mount lens with autofocus feature under natural light illumination.

2.4 Photocatalytic degradation of methyl orange

MO was photocatalytically degraded with TiO_2-NAA-RFs composites of different T_p in a transparent cuvette under simulated solar light irradiation. The TiO_2-NAA-RFs composites, which had an effective area of 1 cm^2, were placed in a cuvette containing a mixture of 2 mL of 5 mg L^{-1} MO and 0.1 M hydrogen peroxide (H_2O_2) solution. The solution was stirred magnetically in a dark vessel (solar simulator) for 30 min to reach the adsorption–desorption equilibrium. After this, simulated solar light irradiation was shined using a 150 W halogen lamp (HL250–A, Amscope, Australia). The absorbance of the absorption peak of MO for each illumination time interval (i.e. 30 min) was analysed by UV-visible spectroscopy to determine the concentration of MO at specific time intervals. The photocatalytic conversion ratio (C_t/C_o), where C_o is the concentration of solution after stirring in the dark for 30 min and C_t is the concentration at illumination time t, was evaluated to determine the kinetic model for this photocatalytic system.

3. RESULTS AND DISCUSSION

3.1 Effect of anodisation parameters on the optical properties of NAA-RFs

The effect of T_P on the characteristic transmission PSB (i.e. 1st order) of NAA-RFs produced by SPA was studied by manipulating T_P from 650 to 850 s with an interval (ΔT_P) of 100 s. Fig. 3a demonstrates that the central wavelength (λ_C) is linearly dependent on T_P at fixed t_{pw} as shown by the slopes of the fitting lines (i.e. 0.55 ± 0.03, 0.49 ± 0.00, 0.44 ± 0.03 and 0.43 ± 0.07 nm s^{-1} for t_{pw} of 0, 2, 4 and 6 min, respectively). Furthermore, the position of the characteristic transmission PSB of NAA-RFs is red-shifted with T_P, in which this effect is also displayed in the interferometric colours of NAA-RFs (Fig. 3b). This phenomenon is due to the relationship between T_P and the period length (L_{TP}) of NAA-RFs[27]. When T_P increases, L_{TP} (i.e. the length of NAA layers between the consecutive sinusoidal pulses)[30] in the photonic structure also increases. As a result, NAA-RFs reflect light more efficiently at longer wavelengths, which is in good agreement with the Bragg's law[27] and previous studies[30]. Therefore, T_P can be manipulated to precisely tune the position of the PSB of NAA-RFs across the entire UV-visible-NIR spectrum and display various interferometric colours of NAA-RFs.

To study the effect of t_{pw} on the position of characteristic transmission peak of NAA-RFs, t_{pw} was varied from 0 to 6 min with an interval of 2 min. As indicated in Fig. 3a, an increase in t_{pw} is accompanied by a decrease in λ_C, implying that the position of the 1st order PSB of NAA-RFs is blue-shifted with t_{pw}, which is in good agreement with previous studies on NAA-RFs[30]. This blue-shift is also featured in the interferometric colours of NAA-RFs as shown in Fig. 3b. The blue-shift observed is associated with the modification of the nanoporous structure of NAA-RFs by wet chemical etching. This process widens the pores of NAA-RFs, which in turn modifies the effective medium of NAA-RFs and alters the PSB. Thus, a pore widening treatment allows the precise tuning of the position of characteristic transmission PSB of NAA-RFs across the spectral regions with various interferometric colours showcased.

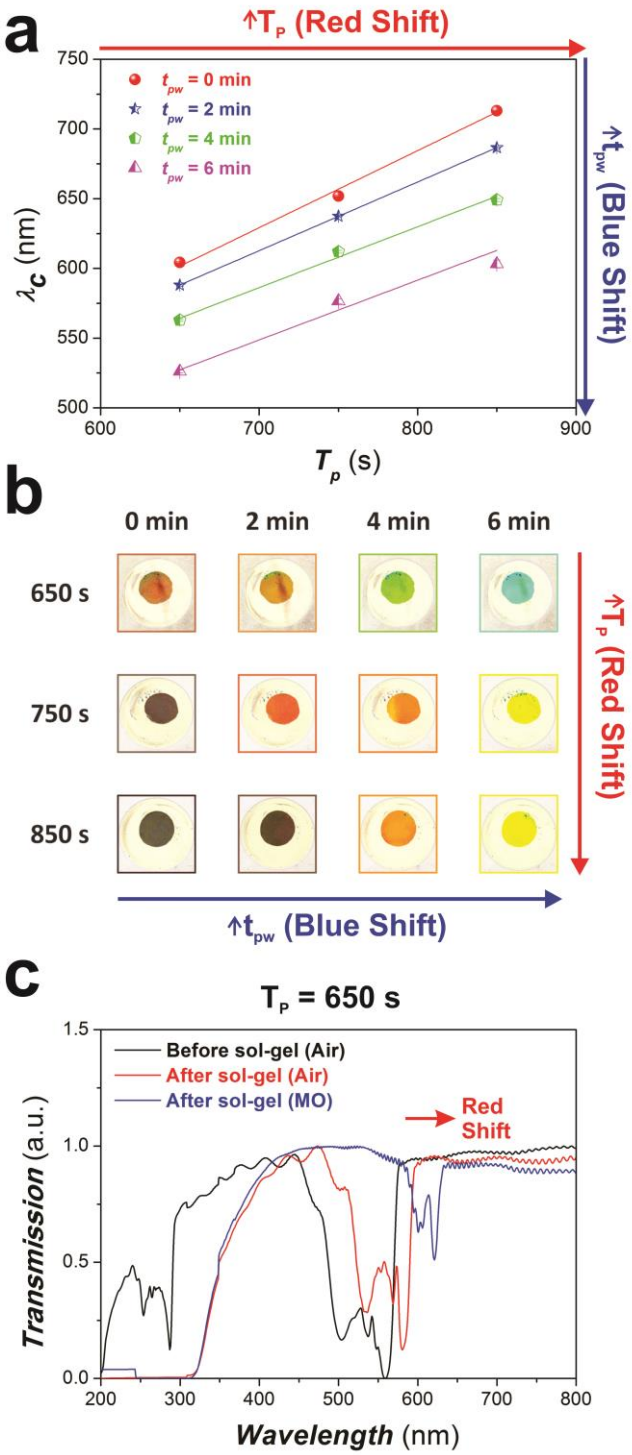

Figure 3. Tunability of the characteristic transmission PSBs and interferometric colours of NAA-RFs by the anodisation and sol-gel parameters. (a) Position of the first characteristic transmission PSB of NAA-RFs as a function of T_P and t_{pw}. (b) Interferometric colour of NAA-RFs as a function of T_P and t_{pw}. (c) Representative transmission spectrum of a reference NAA-RF (i.e. T_P = 650 s, A_J = 0.420 mA cm^{-2}, J_{Offset} = 0.280 mA cm^{-2}, J_{Min} = 0.280 mA cm^{-2}, J_{Max} = 1.12 mA cm^{-2}, t_{An} = 20 h and t_{pw} = 6 min) in air and 5 mg L^{-1} of MO before and after sol-gel modification with TiO_2 for 24 h.

3.2 Effect of surface modification of NAA-RFs with TiO_2

The effect of the surface functionalisation of NAA-RFs (i.e. T_P = 650 s, t_{pw} = 6 min) with TiO_2 layers on the position of the characteristic transmission PSB was studied after the photonic structures was dip-coated with TiO_2 sol for 24 h by sol-gel method. As demonstrated in Fig. 3c, the position of the 1st order PSB with reference to air is red shifted from 526 ± 1 to 556 ± 1 nm after sol-gel modification. A more significant red shift in the position of PSB (i.e. 612 ± 1 nm) is observed when the surface-modified NAA-RF is filled with 5 mg L^{-1} of MO. These red-shift phenomena are observed due to the increase of the refractive index of the medium filling the nanopores of NAA-RFs, including photo-active layers of TiO_2 and MO solution, which both have larger refractive index than that of air. It should also be noted that the full width at half maximum (FWHM) of the PSB decreases after filling the nanopores with TiO_2 and MO solution. This reduction is caused by the light absorption of TiO_2 and MO solution, which filled the nanopores of the NAA-RFs[30, 35]. Besides that, the 2nd order transmission PSB disappears after sol-gel method. This is because the 2nd order PSB is located at positions <300 nm, which corresponds to the strong UV absorption range of TiO_2 (<380 nm)[36]. This indicates that TiO_2 is successfully deposited onto the inner surface of NAA-RFs. Surface-modified NAA-RFs of different T_P (750 and 850 s) with the same t_{pw} (6 min) also showed similar red shifts, reduction in FWHM and disappearance of 2nd order PSB. Therefore, NAA-RFs are proved to be surface-modified with photo-active layers of TiO_2 and their PSB demonstrated to be tunable across the UV-visible-NIR spectrum by manipulating the filling fractions of the medium.

3.3 Photocatalytic degradation of methyl orange with surface-modified NAA-RFs

Photocatalytic degradation of MO as model dye was studied to evaluate the photocatalytic performances of the surface-modified NAA-RFs (T_P = 650, 750 and 850 s; t_{pw} = 6 min) under simulated solar light irradiation. The photocatalytic activity of these NAA-RFs for liquid-phase degradation was carried out with the addition of 0.1 M H_2O_2 solution to aid in the photogeneration of charge carriers in TiO_2. After addition of H_2O_2, the performances of the surface-modified NAA-RFs were measured as displayed in Fig. 4a, where the photocatalytic degradation process is fit for pseudo-first order kinetics by linearising the formula into equation (2):

$$-\ln\left(\frac{C_t}{C_o}\right) = kt \tag{2}$$

In this equation, C_o is the adsorption-desorption equilibrium concentration, C_t is the concentration at time t and k is the apparent rate constant.

The values of k for the MO degradation using surface-modified NAA-RFs with T_P values of 650, 750 and 850 s were 0.31 ± 0.01, 0.36 ± 0.01 and 0.34 ± 0.00 h^{-1}, respectively. These k values are all larger than that for commercial P25 TiO_2 nanoparticles treated with aqueous H_2O_2 solution (i.e. k = 0.24 h^{-1})[37], demonstrating that the surface-modified NAA-RFs perform better than the commercial P25 TiO_2 nanoparticles in the photocatalytic degradation of MO under simulated solar light irradiation (~23–33% enhancement). Besides that, the surface-modified NAA-RF with T_P = 750 s was the most efficient photo-active PC platform to degrade MO. This result can be ascribed to the slow photon (SP) effects, which enhances the photocatalytic degradation of MO. According to Nishimura et al.[26], the light propagated at the vicinity of the PSB will slow down and localise in different parts of the PC structure. The SP will localise in the high dielectric part of the photonic crystal (i.e. photocatalyst) at the red edge of PSB and in the low dielectric part (i.e. dye or voids) at the blue edge of PSB. Therefore, when the edges of the PSB are matched with the absorption peak of the dye, the photocatalytic degradation of the dye can be significantly enhanced. To validate if the increase in the photocatalytic performance of surface-modified NAA-RF (i.e. T_P = 750 s) is due to SP effects, the characteristic transmission PSB of surface-modified NAA-RFs (T_P = 650, 750 and 850 s) with the absorption peak of MO are displayed in Fig.4 (b, c and d respectively). According to this analysis, the blue edge of the PSB of the surface-modified NAA-RF with T_P = 750 s is the nearest to the absorption peak of MO, which corresponds to the best photocatalytic activity observed for MO degradation. This demonstrates that SP effects play a major role in improving the photocatalytic degradation of MO for this type of surface-modified NAA-RF.

Besides that, when the position of the characteristic transmission PSB of surface-modified NAA-RFs is far away from the absorption peak of MO, the photocatalytic degradation of MO should be independent of the PSB[25] and only related to the changes of the overall photonic structures. For instance, with increasing T_P, mass transfer and light utilisation efficiency may have enhanced for light absorption of TiO_2 due to the enlargement of L_{TP} in the NAA-RFs. Consequently,

TiO_2 can generate more ·OH radicals to mineralise MO, increasing the photocatalytic degradation rate. Therefore, since the PSB of the surface-modified NAA-RFs with T_P of 650 and 850 s are far away from the absorption peak of MO (Figs. 4b and d, respectively), it is observed that the photocatalytic performances of the surface-modified NAA-RFs increases with increasing T_P (Fig. 4a). Moreover, the increased light absorption by TiO_2 may also be influenced by the light scattering occurring within the structure of the surface-modified of NAA-RFs with TiO_2. Hence, the changes in the surface-modified NAA-RFs can be significant for the photocatalytic degradation of MO and investigation on the effects of other anodisation and sol-gel parameters should be carried out.

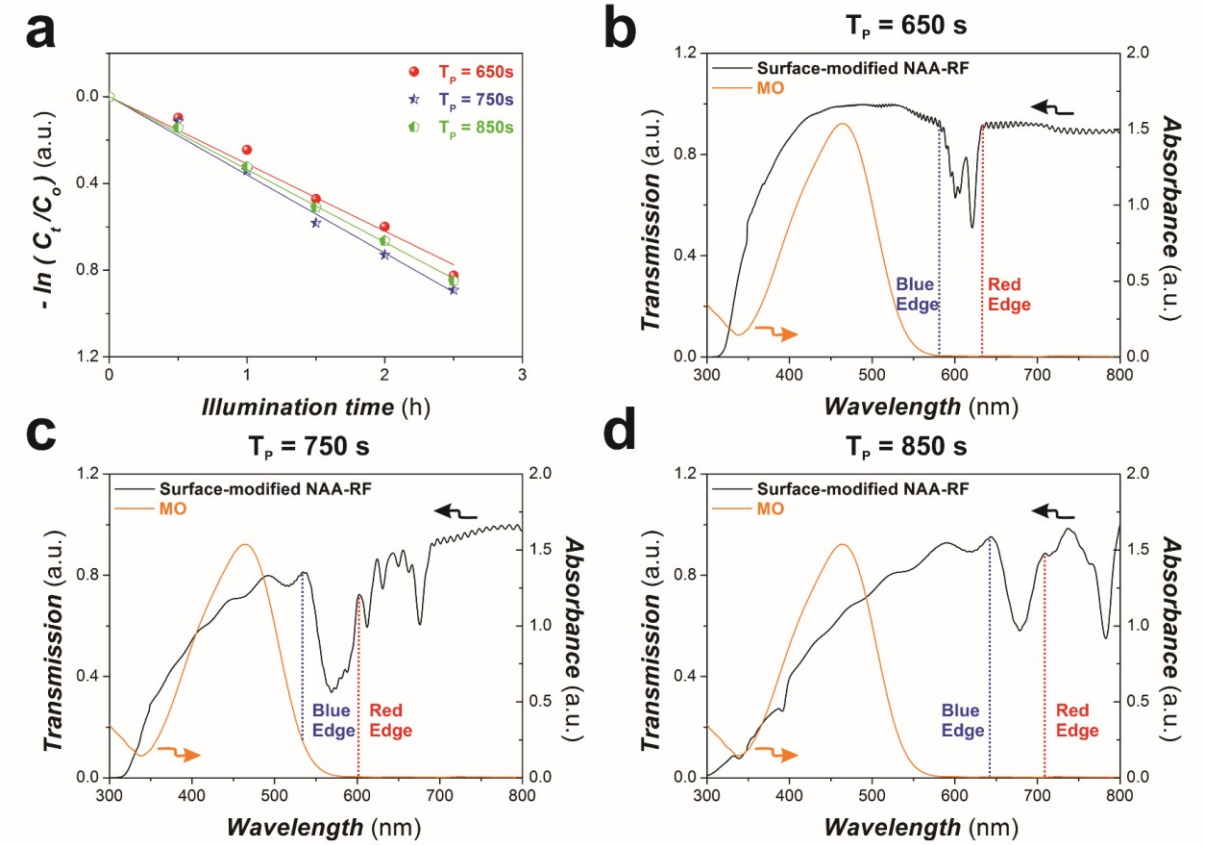

Figure 4. Effect of slow photon effects of the surface-modified NAA-RFs on the photocatalytic degradation of MO. (a) Kinetic linear simulation curve of photocatalytic degradation of MO under simulated solar light irradiation. Optical absorption peak of MO and transmission spectra of TiO_2-NAA-RF composites with an anodisation period of (b) 650 s, (c) 750 s and (d) 850 s.

3.4 Kinetics

A photocatalytic degradation mechanism for the surface-modified NAA-RFs with the addition of H_2O_2 solution is deduced based on the above experiment. When TiO_2 is irradiated with simulated solar light, electron/hole pairs are generated in the conduction and valence band of TiO_2, respectively. Nevertheless, fewer ·OH radicals are produced for the decomposition of organic dye since the photogenerated charge carriers may readily recombine due to short lifetime in the electronic bands. This will result in a slow photocatalytic kinetics. Hence, TiO_2 is deposited on the surfaces of NAA-RFs to utilise the SP effects of the photonic structures to increase the lifetime and photogeneration of the charge carriers. This increase is possible since the photons at the frequency edges of the PSB will propagate with strongly reduced group velocity, being trapped within the photonic structure. Since the slow photons are localised in the edges of PSB, matching these edges with the absorption peak of the organic dye (i.e. localised region of the organic dye) can increase the efficiency of the photocatalytic degradation of TiO_2 in the PC structures to mineralise the organic dye into carbon dioxide and water. Furthermore, H_2O_2 is also added as a primary electron acceptor to facilitate the electron-charge transfer and promote the generation of the ·OH radicals, improving the photocatalytic performances of the surface-

modified NAA-RFs. Thus, the addition of H_2O_2 and the surface modification of NAA-RFs with TiO_2 can enhance the photocatalytic degradation of MO under simulated solar light irradiation.

4. CONCLUSION

In summary, this study has presented an approach to synthesise photonic crystal structures based on NAA and TiO_2 for improving the photocatalytic degradation performances. The optical properties of NAA-RFs (i.e. characteristic PSB) synthesised by sinusoidal pulse anodisation was carried out by systematically modifying two anodisation parameters (i.e. anodisation period and pore widening time) for precise tuning of the PSB across the UV-visible-NIR spectrum. The surfaces of NAA-RFs with different anodisation period (i.e. 650, 750 and 850 s) at fixed pore widening time (i.e. 6 min) were subsequently modified with photo-active layers of TiO_2 by sol-gel method to provide these PCs with photocatalytic properties. When the edges of the PSB of the surface-modified NAA-RF (T_P = 750 s) are matched closely to the absorption peak of the model dye (i.e. MO), the photocatalytic activity of the system is significantly improved due to SP effects in the PC structures. Nevertheless, when the position of PSB of surface-modified NAA-RFs are located away from the absorption peak of dye, the photocatalytic degradation of MO is independent of the PSB and becomes dependent on the period length of the photonic structures since mass transfer and light utilisation enhance with increasing period length (i.e. increasing anodisation period). Therefore, the rationale generated using TiO_2-NAA-RFs PC structures as model composite photocatalyst material may provide new opportunities to develop cost-competitive, simple and sustainable photocatalysts for the photodegradation of persistent organic dyes and pollutants.

REFERENCES

[1] Vaghela, S. S., Jethva, A. D., Mehta, B. B., Dave, S. P., Adimurthy, S. and Ramachandraiah, G., "Laboratory studies of electrochemical treatment of industrial azo dye effluent," Environ. Sci. Technol. 39(8), 2848-2855 (2005).

[2] Prasad, A. R. and Joseph, A., "Synthesis, characterization and investigation of methyl orange dye removal from aqueous solutions using waterborne poly vinyl pyrrolidone (PVP) stabilized poly aniline (PANI) core-shell nanoparticles," RSC Adv. 7(34), 20960-20968 (2017).

[3] Garg, V. K., Amita, M., Kumar, R. and Gupta, R., "Basic dye (methylene blue) removal from simulated wastewater by adsorption using Indian Rosewood sawdust: a timber industry waste," Dyes Pigm. 63(3), 243-250 (2004).

[4] Sun, H., Cao, L. and Lu, L., "Magnetite/reduced graphene oxide nanocomposites: One step solvothermal synthesis and use as a novel platform for removal of dye pollutants," Nano Res. 4(6), 550-562 (2011).

[5] Hai, F. I., Yamamoto, K. and Fukushi, K., "Hybrid treatment systems for dye wastewater," Crit. Rev. Environ. Sci. Technol. 37(4), 315-377 (2007).

[6] Husain, Q., "Potential applications of the oxidoreductive enzymes in the decolorization and detoxification of textile and other synthetic dyes from polluted water: A review," Crit. Rev. Biotechnol. 26(4), 201-221 (2006).

[7] Lee, K., Mazare, A. and Schmuki, P., "One-dimensional titanium dioxide nanomaterials: nanotubes," Chem. Rev. 114(19), 9385-9454 (2014).

[8] Coronado, J. M., Fresno, F., Hernández-Alonso, M. D. and Portela, R., [Design of Advanced Photocatalytic Materials for Energy and Environmental Applications], Springer, London, 85-102 (2013).

[9] Ollis, D. F., Pelizzetti, E. and Serpone, N., "Photocatalyzed destruction of water contaminants," Environ. Sci. Technol. 25(9), 1522-1529 (1991).

[10] Choi, S. K., Kim, S., Lim, S. K. and Park, H., "Photocatalytic comparison of TiO_2 nanoparticles and electrospun TiO_2 nanofibers: Effects of mesoporosity and interparticle charge transfer," J. Phys. Chem. C 114(39), 16475-16480 (2010).

[11] Fox, M. A. and Dulay, M. T., "Heterogeneous photocatalysis," Chem. Rev. 93(1), 341-357 (1993).

[12] Li, F., Jiang, Y., Yu, L., Yang, Z., Hou, T. and Sun, S., "Surface effect of natural zeolite (clinoptilolite) on the photocatalytic activity of TiO_2," Appl. Surf. Sci. 252(5), 1410-1416 (2005).

[13] Wang, C., Shi, H. and Li, Y., "Synthesis and characteristics of natural zeolite supported Fe^{3+}-TiO_2 photocatalysts," Appl. Surf. Sci. 257(15), 6873-6877 (2011).
[14] Dong, H., Zeng, G., Tang, L., Fan, C., Zhang, C., He, X. and He, Y., "An overview on limitations of TiO_2-based particles for photocatalytic degradation of organic pollutants and the corresponding countermeasures," Water Res. 79, 128-146 (2015).
[15] Wang, C., Shi, H. and Li, Y., "Synthesis and characterization of natural zeolite supported Cr-doped TiO_2 photocatalysts," Appl. Surf. Sci. 258(10), 4328-4333 (2012).
[16] Guesh, K., Márquez-Álvarez, C., Chebude, Y. and Diaz, I., "Enhanced photocatalytic activity of supported TiO_2 by selective surface modification of zeolite Y," Appl. Surf. Sci. 378, 473-478 (2016).
[17] Zhu, X., Chang, Y. and Chen, Y., "Toxicity and bioaccumulation of TiO_2 nanoparticles aggregates in Daphnia magna," Chemosphere, 78(3), 209-215 (2010).
[18] Song, B.-S., Noda, S., Asano, T. and Akahane, Y., "Ultra-high-Q photonic double-heterostructure nanocavity," Nat. Mater. 4(3), 207-210 (2005).
[19] Noda, S., Chutinan, A. and Imada, M., "Trapping and emission of photons by a single defect in a photonic bandgap structure," Nature 407(6804), 608-610 (2000).
[20] Akahane, Y., Asano, T., Song, B.-S. and Noda, S., "High-Q photonic nanocavity in a two-dimensional photonic crystal," Nature 425(6961), 944-947 (2003).
[21] Noda, S., Tomoda, K., Yamamoto, N. and Chutinan, A., "Full three-dimensional photonic bandgap crystals at near-infrared wavelengths," Science 289(5479), 604-606 (2000).
[22] López, C., "Materials aspects of photonic crystals," Adv. Mater. 15(20), 1679-1704 (2003).
[23] Raccis, R., Nikoubashman, A., Retsch, M., Jonas, U., Koynov, K., Butt, H.-J., Likos, C. N. and Fytas, G., "Confined diffusion in periodic porous nanostructures," ACS Nano 5(6), 4607-4616 (2011).
[24] Nykypanchuk, D., Strey, H. H. and Hoagland, D. A., "Brownian motion of DNA confined within a two-dimensional array," Science 297(5583), 987-990 (2002).
[25] Zheng, X., Meng, S., Chen, J., Wang, J., Xian, J., Shao, Y., Fu, X. and Li, D., "Titanium dioxide photonic crystals with enhanced photocatalytic activity: Matching photonic band gaps of TiO_2 to the absorption peaks of dyes," J. Phys. Chem. C 117(41), 21263-21273 (2013).
[26] Nishimura, S., Abrams, N., Lewis, B. A., Halaoui, L. I., Mallouk, T. E., Benkstein, K. D., van de Lagemaat, J. and Frank, A. J., "Standing wave enhancement of red absorbance and photocurrent in dye-sensitized titanium dioxide photoelectrodes coupled to photonic crystals," J. Am. Chem. Soc. 125(20), 6306-6310 (2003).
[27] Santos, A., "Nanoporous anodic alumina photonic crystals: fundamentals, developments and perspectives," J. Mater. Chem. C 5(23), 5581-5599 (2017).
[28] Eftekhari, A., [Nanostructured Materials in Electrochemistry], Wiley-VCH, Weinheim, 1-116 (2008).
[29] Lee, W. and Park, S.-J., "Porous anodic aluminum oxide: Anodisation and templated synthesis of functional nanostructures," Chem. Rev. 114(15), 7487-7556 (2014).
[30] Santos, A., Yoo, J. H., Rohatgi, C. V., Kumeria, T., Wang, Y. and Losic, D., "Realisation and advanced engineering of true optical rugate filters based on nanoporous anodic alumina by sinusoidal pulse anodization," Nanoscale 8(3), 1360-1373 (2016).
[31] Kumeria, T., Santos, A. and Losic, D., "Nanoporous anodic alumina platforms: Engineered surface chemistry and structure for optical sensing applications," Sensors 14(7), 11878-11918 (2014).
[32] Wang, Y., Santos, A., Evdokiou, A. and Losic, D., "Rational design of ultra-short anodic alumina nanotubes by short-time pulse anodization," Electrochim. Acta 154, 379-386 (2015).
[33] Santos, A., Formentin, P. Ferré-Borrull, J., Pallarès, J. and Marsal, L. F., "Nanoporous anodic alumina obtained without protective oxide layer by hard anodization," Mater. Lett. 67(1), 296-299 (2012).
[34] Massard, C., Pairis, S., Raspal, V., Sibaud, Y. and Awitor, K., "Fabrication of TiO_2 nanotanks embedded in a nanoporous alumina template," J. Nanomater. 2015, 1-7 (2015).
[35] Kumeria, T., Rahman, M. M., Santos, A., Ferré-Borrull, J., Marsal, L. F. and Losic, D., "Structural and optical nanoengineering of nanoporous anodic alumina rugate filters for real-time and label-free biosensing applications," Anal. Chem. 86(3), 1837-1844 (2014).
[36] Zhang, Z. and Wu, H., "Multiple band light trapping in ultraviolet, visible and near infrared regions with TiO_2 based photonic materials," Chem. Commun. 50(91), 14179-14182 (2014).
[37] Zou, J., Gao, J. and Wang, Y., "Synthesis of highly active H_2O_2-sensitized sulfated titania nanoparticles with a response to visible light," J. Photochem. Photobiol. 202(2-3), 128-135 (2009).